

# Design and acoustic tests of the ATHENA WFI filter wheel assembly development model towards TRL5

Szymon Polak<sup>a,\*</sup>, Jacek Musiał<sup>a</sup>, Robert Pietrzak<sup>a</sup>, Adam Sikorski<sup>a</sup>,  
Mateusz Dumin<sup>a</sup>, Adam Dacko<sup>a</sup>, Mirosław Rataj<sup>a</sup>, Tomasz Barciński<sup>a</sup>,  
Tadeusz Kamisiński<sup>b</sup>, Adam Pilch<sup>b</sup>, Wojciech Binek<sup>b</sup>,  
Grzegorz Woźniak<sup>c</sup>, Monika Zuchniak<sup>c</sup>, Agata Różańska<sup>c</sup>,  
Norbert Meidinger<sup>d</sup>, Marcus Plattner<sup>d</sup>, Jintin Frank<sup>d</sup>, Rafael Strecker<sup>d</sup>,  
Andreas von Kienlin<sup>d</sup>, Marco Barbera<sup>e,f,\*</sup>, Fabio D’Anca<sup>f</sup>,  
Daniele Gulli<sup>f</sup>, Ugo Lo Cicero<sup>f</sup>, Nicola Montinaro<sup>g</sup>, Giancarlo Parodi<sup>h</sup>,  
Enrico Bozzo<sup>i</sup>, and Stephane Paltani<sup>i</sup>

<sup>a</sup>Polish Academy of Sciences, Space Research Centre, Warsaw, Poland

<sup>b</sup>AGH University of Science and Technology, Department of Mechanics and Vibroacoustics, Kraków, Poland

<sup>c</sup>Polish Academy of Sciences, Nicolaus Copernicus Astronomical Center, Warsaw, Poland

<sup>d</sup>Max-Planck-Institut für extraterrestrische Physik, Garching, Germany

<sup>e</sup>Università degli Studi di Palermo, Dipartimento di Fisica e Chimica – Emilio Segrè, Palermo, Italy

<sup>f</sup>INAF-Osservatorio Astronomico di Palermo, Palermo, Italy

<sup>g</sup>Università degli Studi di Palermo, Dipartimento di Ingegneria, Palermo, Italy

<sup>h</sup>BCV progetti s.r.l., Milano, Italy

<sup>i</sup>Université de Genève, Département d’astronomie, Faculté des sciences, Switzerland

**Abstract.** The filter wheel (FW) assembly (FWA), developed by the CBK Institute, is one of the critical subsystems of the wide field imager (WFI) instrument on board the Advanced Telescope for High Energy Astrophysics—mission of the ESA Cosmic Vision 2015-25 space science program (launch scheduled around 2035). The instrument has to collect soft x-rays with very high quantum efficiency, thus WFI requires extremely thin optical blocking filter (OBF). Due to its thickness (~150 nm) and large area (~170 mm × 170 mm) needed to achieve a 40' × 40' instrument field of view, the filter is extremely vulnerable to acoustic loads generated during Ariane 6 rocket launch. On the other side, FW mechanism has to provide high overall reliability, so it is more favourable to launch the instrument in atmospheric pressure (without vacuum enclosure for filter protection). Design efforts of the FW subsystem were focused on two issues: providing maximal possible sound pressure level suppression and smallest possible differential pressure across the OBF, which should prevent filters from damaging. We describe the design of a reconfigurable acoustic-demonstrator model (DM) of WFI FWA created for purposes of acoustic testing. Also, the acoustic test campaign is described: test methodology, test criteria, and results discussion and its implication on future FWA design. In general, tests conducted with the FWA DM showed that current design of WFI is feasible and the project can be continued without introducing a vacuum enclosure, which would significantly increase system complexity and mass. © The Authors. Published by SPIE under a Creative Commons Attribution 4.0 International License. Distribution or reproduction of this work in whole or in part requires full attribution of the original publication, including its DOI. [DOI: [10.1117/1.JATIS.9.2.024002](https://doi.org/10.1117/1.JATIS.9.2.024002)]

**Keywords:** filter wheel; filter wheel mechanism; acoustic tests; advanced telescope for high energy astrophysics; wide field imager; optical blocking filters.

Paper 22083G received Aug. 29, 2022; accepted for publication Mar. 13, 2023; published online Apr. 6, 2023.

\*Address all correspondence to Sz. Polak, [spolak@cbk.waw.pl](mailto:spolak@cbk.waw.pl); Marco Barbera, [marco.barbera@unipa.it](mailto:marco.barbera@unipa.it)

## 1 Introduction

The advanced telescope for high energy astrophysics (ATHENA) is an L-class mission of the Cosmic Vision 2015-25 space science program of the European Space Agency (launch scheduled around 2035). The main goals of this mission would be mapping the hot and energetic phenomena in the Universe with unprecedented telescope effective area, grasp, and spatially resolved high spectral resolution. By performing deep surveys and time resolved high resolution spectroscopy of accretion disks, winds, outflows, and jets, ATHENA will probe black holes at work at different mass scales in shaping the Universe and their surroundings.<sup>1</sup>

This space observatory would be equipped with a single large-aperture x-ray mirror assembly which images x-ray photons onto one of two complementary and interchangeable focal plane instruments: x-ray integral field unit (X-IFU) and wide field imager (WFI).

The X-IFU provides very high spectral resolution by using an array of transition edge sensor micro-calorimeters operated at cryogenic temperatures.<sup>2</sup>

The second instrument - WFI - includes a large detector array (LDA), which covers a field of view of  $40 \times 40$  arcmin<sup>2</sup> and a small fast detector (FD) featuring high count rate capability for the observation of very bright point sources.<sup>3</sup> Both detectors are arrays of depleted p-channel field effect transistors (DEPFETs) silicon active pixel sensors (pixel size  $130 \times 130 \mu\text{m}^2$ ) showing good spectral resolution [full width half maximum (FWHM)  $< 170$  eV @ 7 keV] over the energy band 0.2 to 15 keV together with a high count rate capability (time resolution of 80  $\mu\text{s}$  for the FD and 5 ms for the LDA). Figure 1(a) shows the two detectors of ATHENA mounted on the science instrument module, the selection of the operating instrument is achieved by tilting the telescope. Figure 1(b) shows the schematic layout of the two detector arrays of the WFI, notice that the FD is out of focus to reduce the count-rate per pixel.

The WFI requires filters to reduce visible and ultraviolet light exposure of the DEPFET detector. Separate filters will be mounted on a filter wheel (FW), two thin optical blocking filters (OBF) one for the LDA and one for the FD, and one thick x-ray blocking filter (XBF) for the FD, specifically designed to attenuate the soft emission ( $E < 2$  keV) from x-ray bright sources.<sup>4</sup> The FW will have seven functional positions, namely: (1) both detectors closed, (2) LDA thin OBF, (3) FD thick XBF, (4) both detectors open, (5) LDA calibration (Fe55 radioactive source), (6) FD calibration (Fe55 radioactive source), and (7) FD thin OBF.

The filters, the FW, and the motor gear unit (MGU) make up the FW assembly (FWA).

During launch, the FW will be placed in closed position to provide protection of the detector unit from contamination. This position is also favourable to reduce acoustic load onto the filters which would be placed further away from the entrance baffle, through which acoustic wave would propagate.

To minimize the acoustic noise loads onto the filters, a design effort is needed on the FWA and on the FWA enclosure—top and bottom covers—which is part of WFI primary structure subsystem, which provides structure integrity to the whole instrument. On top of the primary

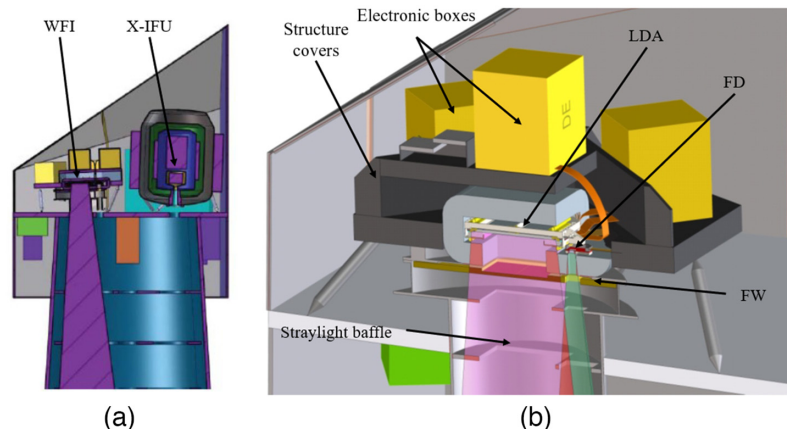


**Fig. 1** (a) Cross-section of ATHENA's science instrument module, with two instruments visible (WFI of left, X-IFU on right). (b) Conceptual design of WFI instrument.

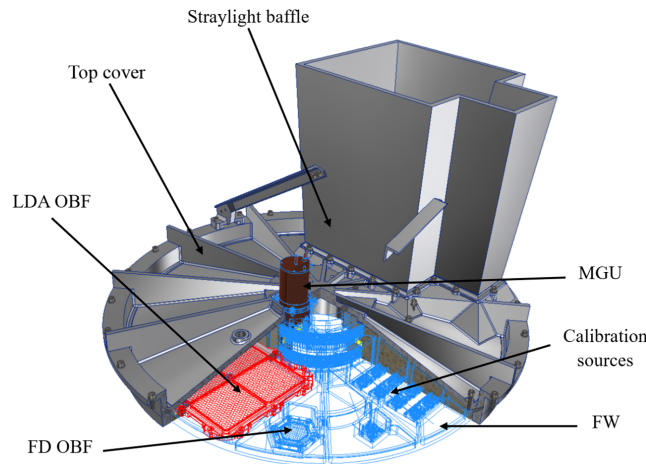


**Fig. 2** WFI FWA isometric view. The LDA OBF is in red while FW, MGU, FD filters, and calibration sources are visible in blue. On top of these components are the cover and straylight baffle.

structure, other critical components are attached, including: the detectors camera head with radiation shielding; the straylight baffle; detector electronic boxes; and mounting legs (see Fig. 1(b) and Fig. 2).

Besides the acoustic noise, filters and FW will be exposed to vibration loads during launch, for this reason the FW will have to provide sufficient structural strength for itself and damping for the filters and other critical components.<sup>5</sup>

In Sec. 2, we describe the WFI acoustic development model, while in Sec. 3 the acoustic test setup. The target OBFs tested are described in Sec. 4 while the two separate acoustic test campaigns performed are described in Secs. 5 and 6. Section 7 provides the results summary and perspectives for future FWA design updates.

## 2 WFI Acoustic Development Model

The WFI FWA acoustic-demonstrator model (A-DM) was built to reproduce the expected acoustic environment around the filters, and to check if the filters are able to survive the acoustic loads in this environment.<sup>6</sup> The geometry of the system has been designed so that it reflects the current state of the project, in particular regarding the closed air volumes and masses of individual elements. Besides the FW itself and MGU mockup (with dummy motor and bearings), other important acoustic components are included: baffle, detector mockup, and top and bottom covers (WFI primary structure mockup) (see Figs. 3 and 4).

For a better simulation of the effects associated with structure vibrations, it was decided to mount the FW through ball bearings, as it would be in target instrument design.

The model was designed with the following functionalities.

- Protection of the model and filters against contamination during acoustic tests by the use of a “Clean tent”—stretched polyethylene film 50  $\mu\text{m}$  thick. The impact of polyethylene film on acoustic performance is negligible in the frequency range of the tests.<sup>7</sup>
- Visual inspection of filters through an acrylic glass windows during tests, to record the moment of potential filter damage, and also to carry out visual inspection of filters “on-site” test area before the model is disassembled in the clean assembly area.
- Ability to modify A-DM structure configurations in order to test the effect of various design changes on acoustic and vibrational response.
- Possibility of placing sensors inside the A-DM to provide information on acoustic and vibration levels in different positions of the model.

The A-DM was mainly made of aluminum alloys to preserve mechanical properties of future target design. To reduce the manufacturing costs and production time, the largest and

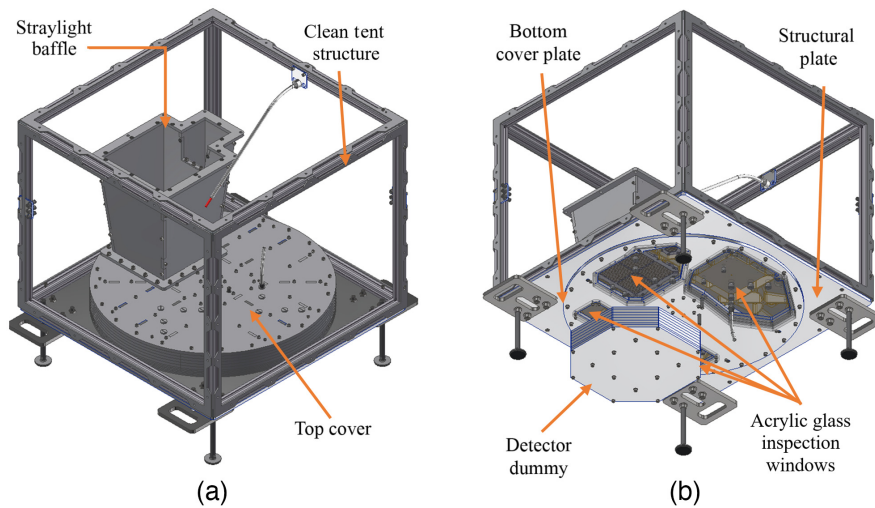


**Fig. 3** Isometric view of the ATHENA WFI A-DM. (a) Isometric “top” view and (b) isometric “bottom” view.

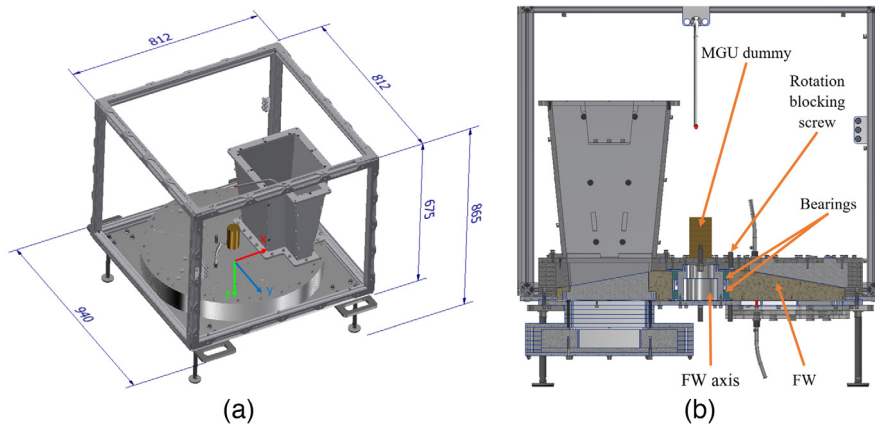


**Fig. 4** (a) Dimensions of A-DM. (b) Cross section view of the A-DM.

least complicated components of the A-DM (baffle, covers, and detector dummy) were built by laser cutting of aluminum sheets, stacked and connected with tightened bolts. To guarantee the proper seal of these elements (baffle, cover, and detector dummy), all edges and boundaries were secured with epoxy glue; seal was tested with water filling.

Two types of sensors were used to gain information about tested system: microphones and accelerometers.

Five microphones were used to get information about the sound pressure level (SPL) and—more important—differential pressure around filter membrane. Two microphones were placed, below and above the LDA filter. A third microphone, used for control of the test load was placed above whole structure inside the clean-tent subsystem. Two more microphones (fourth and fifth) were placed around the tested system, directly in the reverberation chamber, and they were used for control purposes, according to industry standards<sup>8</sup> and ESA’s advices.

Five accelerometers were used to get information about specimen accelerations and displacements. First and second accelerometers were placed on the LDA filter frame (close to FW edge and close to FW bearings). Next two accelerometers were placed on the housing of the

FWA (one on the top side of the cover and one on the acrylic glass cover), around location of LDA filter—this provided data about relative motion of FW with respect to its housing. The fifth accelerometer was placed on a stiff location close to center of the top cover (see Figs. 5 and 6).

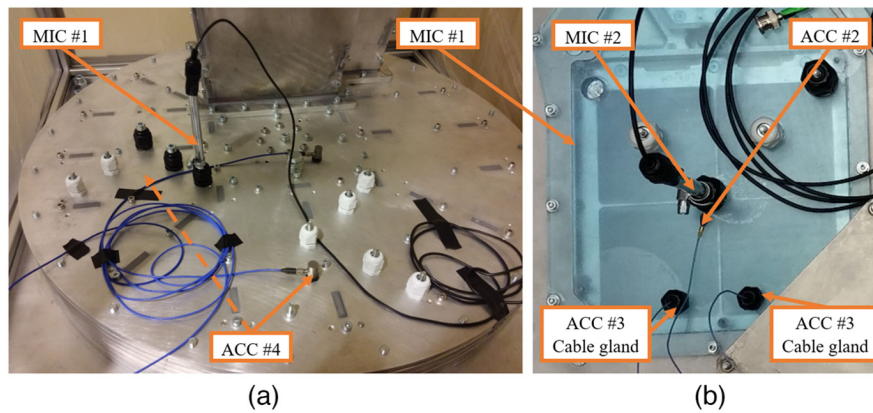


**Fig. 5** A closer look at sensor locations during acoustic tests of WFI acoustic development model. (a) View of the top cover and (b) bottom view (detector side).

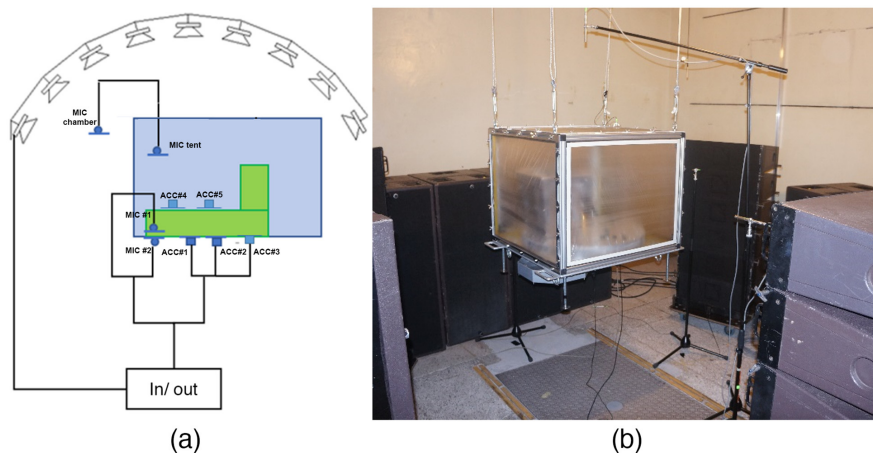


**Fig. 6** (a) Schematic of the test equipment in the reverberation chamber. (b) Photo of the A-DM hanging inside the reverberation chamber, surrounded by loudspeakers.

### 3 Test Campaigns Description

The main purpose of WFI FWA acoustic tests was to evaluate the survivability of WFI filters against the acoustic load during rocket launch. To perform this task, acoustic test campaign was split into two subcampaigns: “dummy” (after use of “dummy” mock-up filter specimens) test campaign in which several issues were checked: test procedures, test linearity and repeatability, measurement sensors best position and—most important—test of several design variants of WFI FWA A-DM, to select acoustically optimal configuration for tests with target filter specimens; and “main” test campaign performed on representative filter breadboards with refined test procedures and with optimal (regarding acoustic load) design configuration.

Both acoustic test campaigns were performed in the Laboratory of Technical Acoustic Science, AGH University of Science and Technology in Krakow, Poland.

#### 3.1 Acoustic Test Setup

To obtain diffused acoustic field conditions, tests were done inside a reverberation chamber with 180 m<sup>3</sup> of volume; with total area of surfaces: 193.6 m<sup>2</sup>; with five diffusing elements and mean reverberation time for mid frequency about 7.5 s.<sup>9</sup>

For test purposes, the A-DM was hung in the center of the reverberation chamber surrounded by the loudspeakers which generated the acoustic load [Fig. 6(b)].

The path of acoustic load signal starts on PC with D/A converter, on which the pink noise was generated, filtered in way to meet Ariane 6 launcher requirements [Fig. 6(a)]. In order to achieve

such acoustic load, signal was amplified by 6x LA8 amplifiers (controlled by Dolby Lake processor) driving a large set of loudspeakers: 18x mid-range loudspeakers [dv-DOSC, 380 W power root mean square (RMS) each], 6x low-range loudspeakers (dv-SUB, 1200 W power RMS each), additional 6x low-range loudspeakers (SB218, 1100 W power RMS each). Combined total RMS power of loudspeakers system was ~20640 W RMS. Loudspeakers were evenly distributed around the A-DM.

### 3.2 Acoustic Load Definition

The target acoustic load spectrum was pink noise filtered to Ariane 6 qualification spectrum according to “Ariane 6 User Manual”.<sup>10</sup> The SPL is defined for each of the first 8 octaves; the overall qualification acoustic SPL is 142.5 dB for a test duration of 120 s (see Table 1).

During dummy tests, the achieved SPL was lower than qualification level (QL) (see Fig. 7: blue line—dummy test level versus green line – QL); however, it was high enough for the purpose of comparing many design variants in order to find the optimal configuration for the “main” tests.

To achieve the technology readiness level 5 required by current ATHENA mission phase, the filter breadboards shall withstand undamaged the Ariane 6 acoustic QL.

**Table 1** Ariane 6 acoustic vibration test levels.

Octave band centre frequency (Hz)	Qualification level (dB)	Protoflight level (dB)	Acceptance level (flight) (dB)	Test tolerance (dB)
	Ref: 0 dB = $2 \times 10^{-5}$ Pascal			
31.5	131	131	128	-2/+4
63	134	134	131	-1/+3
125	139	139	136	-1/+3
250	136	136	133	-1/+3
500	132	132	129	-1/+3
1000	126	126	123	-1/+3
2000	119	119	116	-1/+3
Overall level	142.5	142.5	139.5	
Test duration	2 min	1 min	1 min	

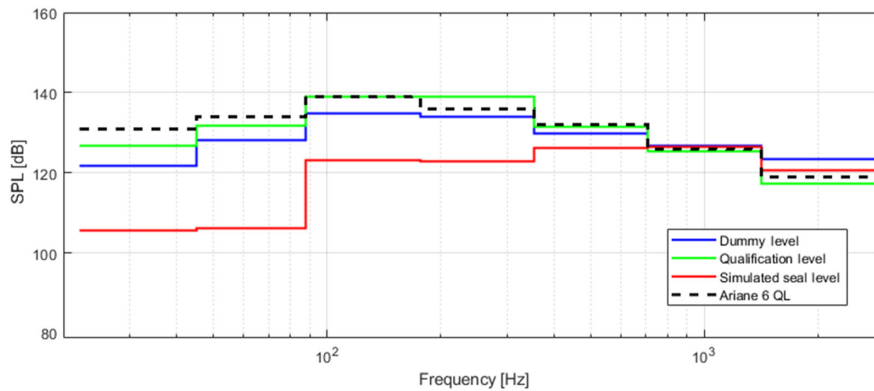


**Fig. 7** SPL load definition curves in “main test campaign”: “qualification level” (green line), “dummy test level” (blue line), “Simulated seal level” (red line). Dashed black line shows reference Ariane 6 QL SPL.

### 3.3 Test Criteria

A large differential pressure across the filter can cause large deformations and stress of the filter membrane, and ultimately its damage. For this reason, the main goal of the “dummy” test campaign was to find the A-DM design configuration that minimizes the differential pressure measured between Mic\_1 and Mic\_2 placed above and below the LDA filter.

The second test criterion was to find the A-DM design configuration, which provides minimal overall SPL around the filter measured by Mic-1.

During “main” tests the main goal was to verify that the LDA filter would survive the applied QL acoustic load.

## 4 Tested Optical Blocking Filters

To satisfy the ATHENA WFI scientific requirement on quantum efficiency (QE), the OBFs shall be very thin ( $\sim 150$  nm thick), for this reason a metal fine mesh with small fraction of blocked area ( $<5\%$ ) is currently baselined to support the thin membrane.

For the purposes of the “dummy” test campaign, dummy filter specimens were manufactured, using free-standing (mesh-less)  $100\text{-}\mu\text{m}$ -thick Mylar foil. The foil has been pre-tensioned to replicate first modal frequencies of target filter. The structural frame is the same, containing the same mounting holes (also for handling tool) and venting canals as the target filter specimen [Fig. 8(a)].

Two target OBF breadboards (also called “main” for testing purposes) were manufactured: the first, named ‘baseline’ design, is made with  $\sim 150\text{-nm}$ -thick polyimide membrane coated with  $\sim 30\text{-nm}$ -thick aluminum layer, and the second one, named “conservative” design, with  $\sim 200\text{-nm}$  polyimide layer and the same amount of Al coating. Both filters are consistent with the WFI QE requirements including detector sensitivity and on-chip OBF transmission ( $\text{QE} > 4.2\% @ 0.2$  keV,  $>78\% @ 1$  keV,  $>89\% @ 7$  keV). The use of the thinner filter would provide a gain in QE of  $\sim 0.3\% @ 0.2$  keV,  $\sim 4\% @ 0.35$  keV (above the C K edge), and  $\sim 1.6\% @ 1$  keV, while the gain at 7 keV is negligible.

The clean aperture of these filters is  $164 \times 164$  mm<sup>2</sup>, the filter is supported by a Au plated stainless steel honeycomb mesh with  $\sim 5\text{-mm}$  pitch ( $150$   $\mu\text{m}$  thick,  $85$   $\mu\text{m}$  wire width including Au plating) and by a cross-shaped structure which divides the filter in four quadrants.

Due to the extremely thin and fragile membrane of this filter, a very careful handling and clean environment is needed—for these purposes an ISO-8 Clean Room environment has been used for A-DM assembly activities, while the polyethylene film tent was used to protect the system during tests inside the reverberation chamber (Fig. 6).

Beside the LDA and FD thin OBFs, a FD thick XBF, consisting of a meshless  $25\text{-}\mu\text{m}$ -thick polyimide film coated with a  $100\text{-nm}$ -thick aluminum layer, has been tested. Due to its increased thickness and smaller size, this filter is less prone to damage under vibroacoustic loads. More information about the tested filter breadboards can be found in Barbera et al. 2018.<sup>10</sup>

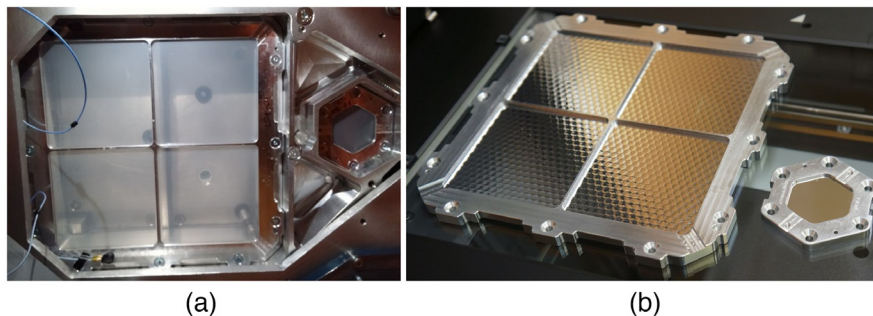


**Fig. 8** (a) Dummy filters attached to A-DM FW—made up of a transparent Mylar foil without mesh. (b) Target aluminized thin polyimide filters supported by a hexagonal pattern fine metal mesh.

## 5 ‘Dummy’ Test Campaign

The initial test campaign named “dummy” was performed mounting inside the FWA A-DM OBF specimens manufactured by UNIPA with a  $\sim 100\text{-}\mu\text{m}$ -thick meshless Mylar foil, which is much stronger and cheaper than target filter. The Mylar foil was pre-stressed to get the first modal frequency @  $\sim 100\text{ Hz}$  similar to the target filter, thus allowing good estimation of test system behaviour.

The main purposes of this test campaign were as follows.

- To check the readiness of the “main” test set-up: manufactured A-DM, clean room area, loudspeakers and amplifiers, measurement apparatus (microphones and accelerometers), and data collecting software.
- To prepare correctly defined acoustic load spectra for test with target filter breadboard.
- To estimate the actual load levels acting on the filters.
- To check impact of A-DM design changes on acoustic performances and identify optimal design configuration.

To fulfil test purposes, the “dummy” test campaign was divided into two sessions.

1. Test set-up readiness verification;
2. A-DM design optimization.

Detailed results of the first part of the “dummy” test campaign are reported in the test report, which will be part of the documentation delivered to ESA for the technical readiness assessment of critical items before mission adoption. For the purpose of this paper we report here only the most meaningful results of the second part of this campaign, which was crucial for the implementation of the “main” test campaign. In particular, different A-DM configurations have been tested.

### 5.1 Tested A-DM Design Configurations

#### 5.1.1 Design variable – balanced versus unbalanced

FW configuration is defined by arrangement of functional positions. It can be arranged in few ways, but from a mechanical point of view, the significant arrangements are related with the location of most massive components, namely the calibration sources and the closed position. Thus, two main design configurations were investigated in which these heavy components are located on the opposite side of FW (“balanced” configuration); or next to each other (“unbalanced” configuration) (Fig. 9). Because the wheel is in the “closed” position during rocket launch, a change in configuration causes a change in the “launch” position of the thin OBFs.

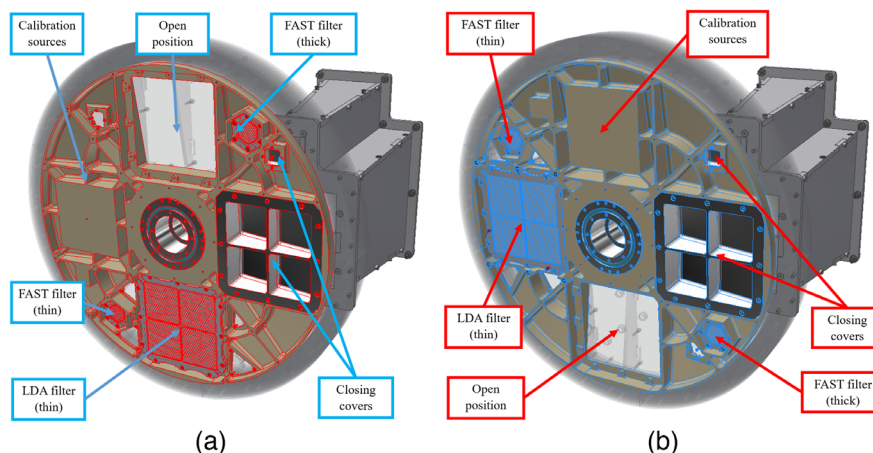


**Fig. 9** “Balanced” configuration (a) and “unbalanced” configuration (b) of the FW.

In “unbalanced” configuration the LDA OBF can be placed either adjacent to or on the opposite side of the closed position (baffle entrance) [Fig. 9(b)]. Both configurations have been tested.

### 5.1.2 Design variable – air gap between FW and its cover

The air-gap between the top-and-bottom covers and the FW determines the air volume through which acoustic waves can propagate from the baffle inside the FWA. Change of this variable was achieved by adding spacers (aluminum rings) in two locations: above-and-below FW Axis and between two sides of the cover (Fig. 10(a)). In total, three configurations were analyzed: no gap increase (+0 mm); small gap increase (+3 mm); and large gap increase (+5 mm).

The results show that the best suppression of acoustic waves inside FWA volume (total SPL and differential pressure) occur with implementation of the smallest possible gap. The influence of this design variable is very high—increasing the gap by 5 mm caused increase of pressures by even 100% (see Fig. 13).

### 5.1.3 Design variable – extended volume around filter

This test covered the impact of extended air volume between thin filters and acrylic glass cover [Fig. 10(b)]. Extended volume was achieved by adding acrylic glass spacers allowing to explore a filter-cover distance in the range from 2 mm (no spacers) up to 32 mm.

The increase of air volume around the filter has a small, but visible impact on reducing the differential pressure and SPL by ~25%. The most likely explanation of this effect is that the increased air volume below filters makes the air volumes above and below filters more equalized and therefore pressures in both regions have similar values. When one volume is much smaller than the other one, then the same incoming acoustic energy in less volume would cause pressure increase, and this causes higher differential pressure. After equalizing volumes around the filter, the acoustic fields above and below filter are more similar and therefore differential pressure is lower and filter membrane is subjected to less deformation.

### 5.1.4 Design variable – opened/closed/sealed baffle

This design variant was achieved by attaching a 10-mm-thick aluminum cover to the baffle entrance. This design variant has been checked only for test purposes and it is not applicable in target WFI FW design, due to increased system complexity and risk related with an additional “baffle door” mechanism.

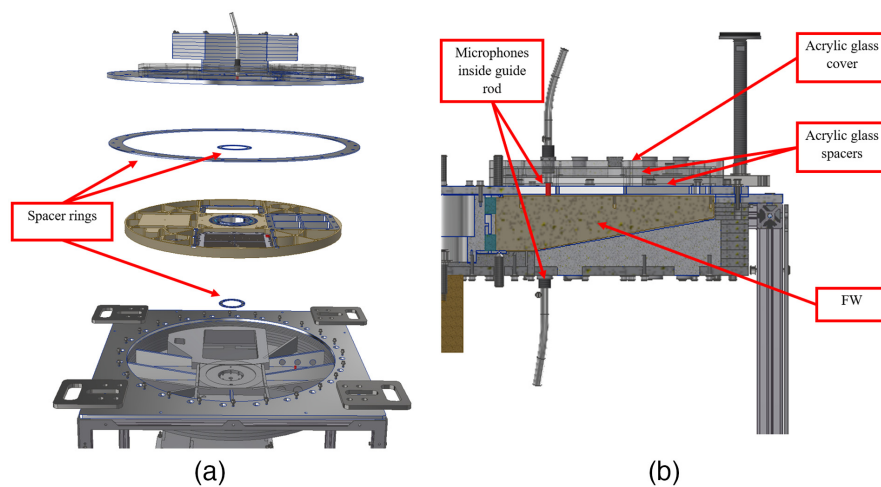


**Fig. 10** Design variables with positive impact on reducing the differential pressure on WFI filters: (a) distance rings for air-gap increment and (b) increased air volume around the thin filters by adding acrylic glass spacers (cross-section view of A-DM).

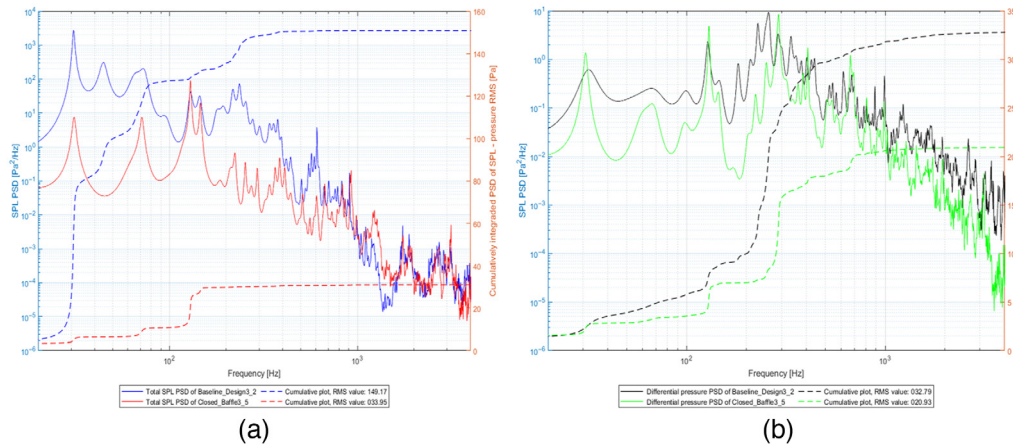


**Fig. 11** (a) Comparison between measured SPL PSD values of Mic1 sensor on baseline design configuration 3.2 (blue solid line) versus the configuration with closed baffle 3.5 (red solid line). (b) Comparison between the differential pressure PSD above and below LDA filter on baseline design configuration 3.2 (black solid line) versus the configuration with closed baffle 3.5 (green solid line). Dashed lines in the two plots provide the cumulative spectra.

This configuration results in a significant reduction in the total SPL (around 4.4 times), with a moderate reduction of differential pressure (~30%). This is most likely due to the baffle-cover frequency response, which dampened the low frequency acoustic load (below 130 Hz), the range responsible for most of the SPL, but it shifted up the 200 to 300 Hz range load responsible for most of the differential pressure (see Fig. 11). The baffle cover cuts off the acoustic wave entering the baffle, but it also acts as a secondary sound source since it may be excited at its resonance frequencies by the outside acoustic field.

### 5.1.5 Design variable – additional venting holes applied

Several closable venting holes (VHs) were introduced into A-DM design to improve pressure equalization above and below filter, either on the side of cover ribs around LDA filter (Fig. 12, right panel) or on the FW structure in vicinity to the LDA filter [Fig. 12(a)]. Introduced VHs may open paths for the stray-light to reach the detector; avoiding stray-light is beyond the scope of the A-DM design, however, future and more advanced designs of the FW will take this issue into account. Opening of the VHs did not have a big impact on total SPL; however, it radically reduced the differential SPL by 45% to 60%, depending on the specific configuration.

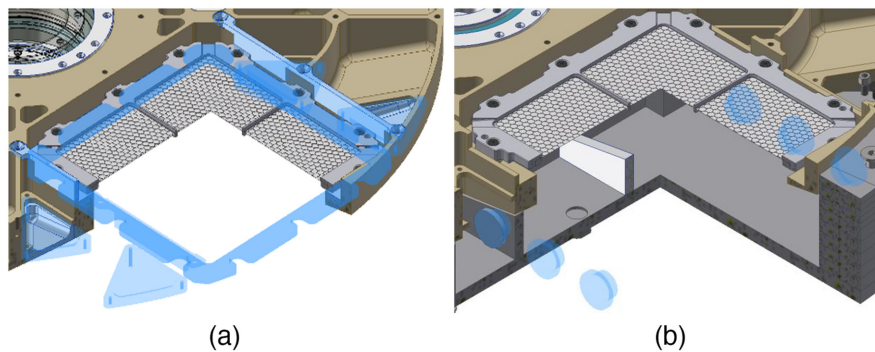


**Fig. 12** (a) Closable VHs on the FW structure around the LDA OBF (all FilterWheel-Closed/all FilterWheel-Opened/only Filter-Frame-Opened (Fc/Fo/F.fr.o in Fig. 13). and (b) closable VHs in FW cover ribs (Cover-Closed/Cover-Opened (Cc/Co in Fig. 13).

### 5.1.6 Design variable – pin-puller simulation

During all tests, a fixing bolt for locking the rotational degree of freedom of the FW was applied. The cone point screw was tightened to the FW near bearing area, causing its additional preloading. In addition, 8× “fixing bolts,” equally distributed on the FW edge were prepared for testing the impact of FW vibrations on the system’s acoustic behaviour. Results show that even with a large reduction by 33% of FW accelerations, the acoustic response of system remained on the level very close to that one of the baseline configuration design. This means that air-vibrations caused by FW excitation do not have any significant impact on the SPL and again—most of the acoustic load received by filters comes from outside the instrument.

### 5.1.7 Design variable – baffle removed

By removing the baffle from FW cover, we investigated its impact on the acoustic field around filters. Baffle removal caused slight reduction of total SPL and differential pressure SPL showing that baffle acts as acoustic amplifier to the system.

## 5.2 Dummy Test Campaign Results Summary

In total, 36 test cases were put into comparison. Figure 13 summarizes the main results of the dummy test campaign.

The design variable with the largest impact on the differential pressure level is the air gap between FW and FW cover. In baseline design configuration, this gap has a value of 1 mm near FW axis and it is linearly increasing up to 2.8 mm near the edge (to ensure that FW edge will not

Test #	FW Bal. / Unbal.	[B]affle / PinPuller	Gap increase [mm]	Vent. Holes	Add Air Volume	prs1	prs2	prs3 (MicTent)	prs4 (MicCham)	dprs
3-3	B	B on	5	Cc-Fe	0	281.3	275.7	212.6	173.0	57.2
3-3	B	B on	3	Cc-Fe	0	246.3	232.1	213.1	174.6	54.4
4-3	U	B on	3	Cc-Fe	0	310.0	290.2	215.4	191.6	49.9
4-3	U	B on	5	Cc-Fe	0	343.2	324.3	206.4	189.6	47.9
3-7	B	B on PP	0	Cc-Fe	0	146.9	143.7	213.0	-	34.2
3-2	B	B on	0	Cc-Fe	0	149.2	146.2	200.6	174.7	32.8
4-2	U	B on	0	Cc-Fe	0	165.6	154.4	216.4	188.3	31.0
3-10	B	B off	0	Cc-Fe	0	136.1	127.9	203.0	-	27.5
3-4	B	B on	0	Cc-Fe	30	140.8	136.3	197.5	173.5	24.9
4-4	U	B on	0	Cc-Fe	30	147.6	138.3	214.0	189.9	22.4
3-5	B	B Closed	0	Cc-Fe	0	33.9	32.9	198.5	173.7	20.9
4-6	U	B on	0	Cc-F.fr.o	0	169.4	158.7	212.9	187.7	17.1
4-6	U	B on	0	Co-Fo	0	177.6	167.7	216.8	187.9	16.4
3-6	B	B on	0	Cc-Fe	0	148.4	143.4	212.0	-	16.0
3-6	B	B on	0	Cc-Fe	0	147.7	139.6	215.2	-	15.3
5-3	B	B on	0	Cc-F.fr.o	30	138.8	134.4	209.9	189.4	14.1
3-6	B	B on	0	Co-Fo	0	141.0	135.9	214.8	-	12.8
5-2	B	B on	0	Co-Fo	20	149.9	143.1	211.1	190.4	12.1
5-1	B	B on	0	Co-Fo	30	145.1	138.8	213.5	191.1	11.6
5-4	B	B Seal	0	Cc-F.fr.c	30	20.6	21.8	212.2	188.2	8.2

(a)

(b)

**Fig. 13** Summary table of the results from the “dummy” acoustic test campaign. First column is the test number, the next five columns describe tested A-DM configurations. Tested configurations are sorted from highest to lowest measured differential pressure across LDA OBF. Pressure RMS values are all in Pascals. Test cases 3-2 and 4-2 marked with thick red frames are the “baseline” configurations (balanced and unbalanced) to which the other cases can be referenced. Colour bars added for increased readability—normalized for prs1-prs4 (pressure values for Mic1: Mic4) columns and separately normalized for dprs (differential pressure between Mic1 and Mic2).

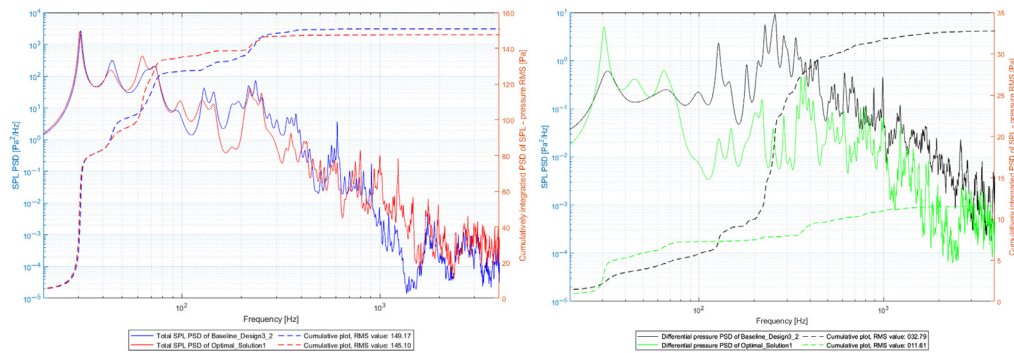


**Fig. 14** (a) Comparison between SPL PSD values of Mic1 sensor on baseline model (blue line) versus optimal model (red line). (b) Comparison between differential pressure PSD above and below LDA filters on baseline model (black line) versus optimal model (green line). Dashed lines in the two plots provide the cumulative spectra.

collide with FW cover during launch vibrations). Increase of this gap from 2.8 mm near edge to 5.8 mm results with 66% increase of differential pressure value. Therefore, air-gap between FW and its cover should be kept as small as possible.

The design configuration with best acoustic performances to be used for the “main” filter tests, named “optimal solution 1,” is a combination of design variables that showed positive impact on reducing the differential pressure onto the LDA filter, namely, balanced FW configuration, minimal air-gap between FW and cover, additional air-volume around filter, opened VHs. Figure 14 shows optimal solution 1 design variant acoustic performance compared with the baseline design configuration. The biggest difference in SPL and differential pressure occurs in the 200 to 400 Hz range.

The lowest differential pressure during “dummy” filter test campaign was registered for the “optimal design 1” configuration with the addition of a seal-putty applied under baffle – between top cover and FW. This test results show the limit of possible reduction of total SPL and differential pressure around filters with the current A-DM FWA design; however, the introduction of such seal would require the usage of a complicated mechanism.

Worth noting are the results of “baffle closed” design variant showing low SPL while the differential pressure is not reduced by the same multiplier. In such configuration, complex acoustic phenomena occurred and its detail description and understanding would require further testing and/or detailed numerical simulations.

Only these two design changes—applying a seal under baffle and closing the baffle—provide big change in spectrum below 100 Hz – in all other test cases the SPL registered near Filters is higher than the control signal, which means that A-DM structure amplifies these low-frequency loads.

## 6 ‘Main’ Test Campaign with Target Filter Breadboards

One month after the “dummy” test campaign, with results analyzed and design-wise decision made, the “main” test campaign was performed with target filter breadboards.

### 6.1 Acoustic Load Levels

During the main test campaign, three load levels were used. The first one called “dummy” (blue curve in Fig. 7) has been introduced to verify the behaviour of the system with the reduced acoustic noise level used in the “dummy” test campaign to check that the system has been correctly prepared for tests.

The second load level—called “Simulated Seal” has been obtained with proper filtering to provide on microphone Mic\_1 a signal equivalent to that one that would be obtained using the seal-putty, which could not be used due to contamination risk on filter breadboards. This load

case has been used to open the door to an intermediate WFI FWA configuration which would still allow the filters to be launched in atmospheric pressure, but would require an extended design effort. In case of filter failure under this reduced load, the whole instrument would have to be redesigned to enclose filters in a vacuum chamber.

The third load case was Ariane 6 “Qualification Level” (green curve in Fig. 7).

## 6.2 Tested Configurations Description

During this test campaign the “optimal solution 1” design variant, described in Sec. 5.2 was used as A-DM configuration for target filter tests, offering maximal protection of filters against acoustic vibration load.

To minimize risks on filters, it was decided to not place any accelerometers in vicinity of filters, therefore, only one accelerometer was placed on A-DM, but on a different position with respect to the “dummy” tests. Beside the lack of accelerometers, A-DM configuration was identical as the one selected in “dummy” filter test campaign.

Two versions of the filters have been tested, the “baseline” based on a polyimide film 150-nm-thick coated with 30 nm of aluminum, and a “conservative” one with a thicker (200 nm) and thus more robust polyimide film with the same amount of aluminum coating.

After completion of the acoustic tests with Ariane 6 QL load on both sets of filters, the same filters have been tested again inside the A-DM setup in a different configuration, hereafter named “stress” corresponding to unbalanced FW configuration without extended air-volume below the filters. The reason behind introducing such load case was to check if filters can survive in acoustically less advantageous configuration, which may be favourable due to other reasons by the WFI team. Also, if filters damage would occur, the knowledge about limit stress would be achieved.

## 6.3 Test Results Summary

Table on Fig. 15 summarizes the RMS pressures measured in all microphones and the RMS differential pressure (last column) across the LDA filter measured by use of microphones prs1 and prs2.

The measurements performed by microphones prs1 and prs2, across LDA filter, in “stress” configuration show total SPL values around 70% higher and around 86% higher for differential pressure SPL with respect to “optimal” configuration.

The measured differential SPL (last column in table) depends on filter specimen under test, likely related with filter membrane thickness: the thinner the filter, the smaller is the registered differential pressure with the highest value occurring for the dummy filter specimen (see Fig. 16). These differences occur for frequencies >150 Hz.

All 200-nm-thick filter specimens (“conservative” design) successfully passed all test loads, in both FWA configurations “optimal” and “stress”—example of achieved loads can be seen in Fig. 17. After each test, filters were visually inspected, and at the end of the test sequence high-resolution images of the filters have been taken in transmission and reflection mode, by use of a high resolution photographic scanner, to search for imperfections. No damage has been reported on this set of filters.

The LDA filter breadboard with 150-nm-thick polyimide (“baseline” design) has passed all tests in “optimal” configuration. This and the previous results conducted on “conservative” filter breadboards confirm that the ATHENA WFI can be launched in atmospheric pressure without vacuum enclosure

The LDA filter “baseline” breadboards have also been tested in “stress” design configuration. After this test, three damaged mesh cells have been recorded (see Fig. 18).

To verify whether the damage was caused by fatigue of the filter, which had already been tested in “optimal” configuration, we have repeated for a second time the acoustic qualification test in “stress” configuration. No further damaged cells have been identified on the filter; neither the present damage has developed to other close by mesh cells. This result strongly suggests that the damage is related to a local filter defect more than to a poor design or technology—probably not fully glued surface interface between filter membrane and mesh. More details on the investigation of the observed damage and failure modeling will be discussed elsewhere.<sup>11</sup>

Test #	LDA Filter	FAST Thin Filter	FAST Thick Filter	FW Design Variant	Load Level	prs1 (above filter)	prs2 (below filter)	prs3 (MicTent)	prs4 (reverb. Chamber)	prs5 (reverb. Chamber)	prs6 (reverb. Chamber)	dprs
#7_1	Dummy	Dummy	Dummy	Stressed	Qualification	210.1	208.0	283.7	211.0	245.4	240.6	55.3
#7_1	Dummy	Dummy	Dummy	Optimal	Qualification	145.0	143.3	278.3	206.0	239.5	233.2	26.4
#7_1	Dummy	Dummy	Dummy	Stressed	Dummy tests	148.1	143.2	178.8	150.2	165.0	154.0	21.3
#7_1	Dummy	Dummy	Dummy	Optimal	Dummy tests	104.8	103.3	178.0	148.4	163.4	152.2	19.1
#7_2	Main 200nm	Main 200nm	Main 25nm	Optimal	Qualification	147.7	141.9	281.1	206.5	240.6	239.6	36.5
#7_2	Main 200nm	Main 200nm	Main 25nm	Optimal	Closed Baffle sim.	24.5	25.2	74.3	82.0	85.3	67.9	7.9
#7_3	Main 150nm	Main 150nm	Dummy	Optimal	Qualification	146.5	145.0	278.6	209.5	238.2	236.1	42.0
#7_3	Main 150nm	Main 150nm	Dummy	Optimal	Closed Baffle sim.	25.8	26.6	76.0	83.3	85.0	66.0	8.6
#7_4	Main 2 150nm	Dummy	Dummy	Optimal	Qualification	144.7	142.9	280.9	207.8	239.1	238.2	22.5
#7_4	Main 2 150nm	Dummy	Dummy	Optimal	Closed Baffle sim.	25.0	26.0	74.9	83.2	85.5	66.4	15.2
#7_5	Main 3 150nm	Dummy	Dummy	Optimal	Qualification	144.3	144.4	281.5	208.8	238.0	237.7	27.9
#7_5	Main 3 150nm	Dummy	Dummy	Optimal	Closed Baffle sim.	25.6	26.2	75.2	82.5	85.3	64.5	16.8
#7_6	Dummy	Dummy	Dummy	Stressed	Qualification	252.8	249.1	270.8	222.9	223.2	227.0	99.3
#7_6	Dummy	Dummy	Dummy	Stressed	Closed Baffle sim.	50.7	50.1	73.3	83.4	69.5	62.8	11.9
#7_7	Main 200nm	Main 200nm	Dummy	Stressed	Qualification	263.7	262.5	285.4	209.8	239.8	240.3	67.4
#7_7	Main 200nm	Main 200nm	Dummy	Stressed	Closed Baffle sim.	56.1	53.3	74.1	83.6	85.5	66.8	8.6
#7_8	Main 150nm	Main 150nm	Dummy	Stressed	Qualification	261.2	264.9	284.5	208.9	240.3	238.2	68.7
#7_8	Main 150nm	Main 150nm	Dummy	Stressed	Qualification	258.4	258.7	280.0	231.9	238.3	237.1	50.4
#7_8	Main 150nm	Main 150nm	Dummy	Stressed	Closed Baffle sim.	55.9	53.4	75.2	83.2	86.2	65.4	7.5
#7_9	NoFilter	Dummy	Dummy	Stressed	Qualification	263.5	253.7	281.4	207.6	239.6	237.8	16.2
#7_10	NoFilter	Dummy	Dummy	stressed, No Test	Qualification	265.6	255.8	284.0	210.0	239.0	238.8	16.5

(a)

(b)

**Fig. 15** Table of measured RMS pressure values in “main” tests. (a) A-DM configuration, set of filters under test, and acoustic load level. (b) RMS pressure value measured on each sensor, and—in the last column—the RMS differential pressure across the LDA filter. All pressures are in Pascals.

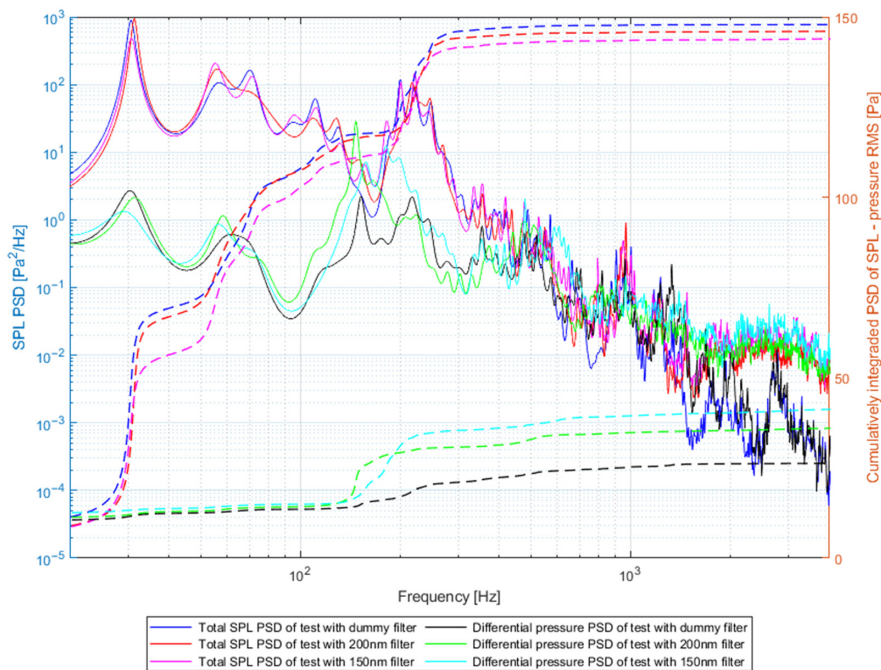


**Fig. 16** Comparison between LDA filter thickness under same “optimal” load (Tests #7\_1, #7\_2 and #7\_3).

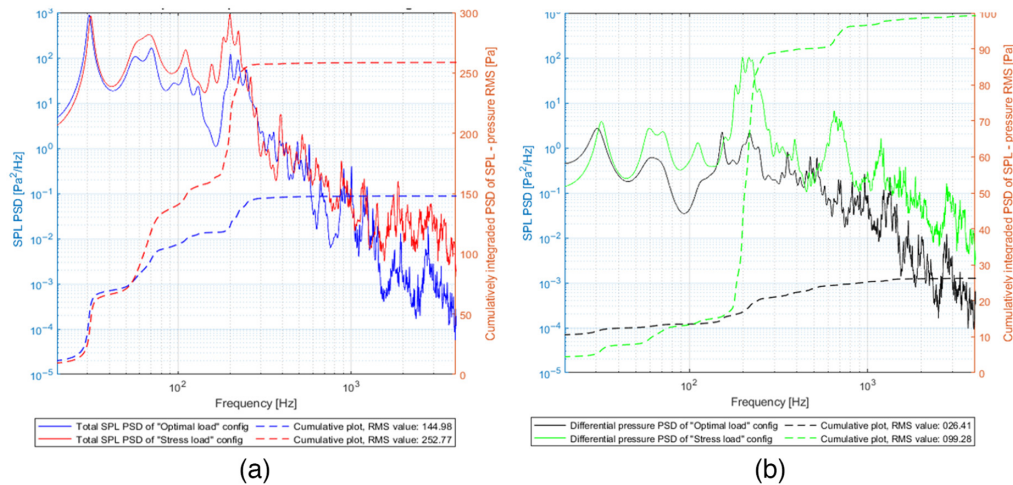


**Fig. 17** (a) Comparison between total SPL PSD values of Mic1 sensor on optimal configuration (blue line) versus stress configuration (red line). (b) Comparison between differential pressure PSD above and below LAD filters on optimal configuration (black line) versus stress configuration (green line). Dashed lines in the two plots provide the cumulative spectra.

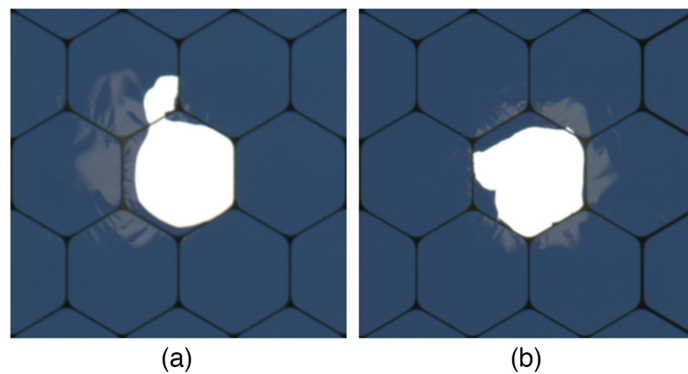


**Fig. 18** (a) and (b) Photographic scanner images showing the three cells where the thin polyimide/al membrane of the “baseline” filter has broken after the “stress” acoustic test. The honeycomb mesh pitch is  $\sim 5$  mm.

## 7 Summary and Conclusions

The design consolidation of the ATHENA mission and its science instruments require severe qualification activities, already in early stages of development. Unique and already proven technologies require extensive design, analysis, and test efforts to make sure that they can be reliably used in space.

The FWA is considered a critical item in the ATHENA WFI since it has to reliably control the detector operation configuration (open, closed, calibration, and filter) and to guarantee the safety of the fragile OBFs. In fact, the FWA shapes the acoustic noise environment of the filters during launch and controls the evacuation rate occurring in few minutes during the lift-off.

In this paper, we report results from two extensive acoustic test campaigns performed at AGH University in Krakow within the design consolidation and technology demonstration activities performed in the phase B of the ATHENA mission.

In the first test campaign, named “dummy” by the use of dummy filters in place of representative fragile breadboards, a large number of configurations of a FWA development model have been investigated. The following design variables have been identified to have positive impact on reducing the differential pressure across the filters in a simulated Ariane 6 launch acoustic environment (arranged from highest to lowest impact).

- Seal under the straylight baffle.
- Straylight baffle closure.
- Thickness reduction of gap between FW and the FW cover,
- Opening VHS in FW cover and in FW around filter area
- Increasing the air volumes around filters.
- Ribbed inner side of WFI primary structure around FW.

The implementation of the first two design variables into the target WFI design may add single point of failure and reduce the overall system reliability. However, it may be used as a backup solution before introduction of vacuum enclosure of the whole instrument.

The gap size between FW and WFI primary structure has to be minimized. This has a large impact on the mechanical design requiring a FW-bearings system stiff enough to avoid clash during launch vibrations.

The three last design variables should be all implemented in the next FWA design iterations. The exact shape and size of used VHS, ribs location (which creates air pockets) and additional air-volume near filters can be estimated using design optimization techniques with acoustic numerical simulations.<sup>12</sup>

It is important to point out that is that the SPL recorded near the filters is amplified by the A-DM structure with respect to control signal at frequencies below 60-100 Hz. This effect can be reduced only by big changes in the structure (e.g., closing the baffle and seal under baffle).

The second acoustic test campaign, named “main” by the use of the representative filter breadboards has been performed to prove that filters can survive the Ariane 6 launch acoustic environment. For this campaign the FWA demonstration model has been setup in the so called “optimal configuration 1” minimizing the differential pressure across the filters. A second FWA setup named “stress” configuration has also been tested providing higher acoustic load acting on filters.

Two types of filters have been tested, namely: the “baseline” design with the polyimide membrane 150 nm thick and the “conservative” design with a 200-nm-thick polyimide film.

The main conclusions of the “main” test campaign are as follows.

- The current investigated design and technology of the WFI OBFs can withstand the Ariane 6 launcher acoustic load inside the FWA.
- It is possible to launch the WFI in atmospheric pressure, without a vacuum enclosure for filter protection.
- The 200-nm-thick “conservative” design filters have passed the acoustic qualification tests both in FWA “optimal” and “stress” design configurations.
- The 150-nm-thick “baseline” design filters have passed the acoustic qualification tests in FWA “optimal” design configuration, while presented a localized damage of few membrane cells under “stress” test. The damage seems to be related to local filter defect more than a poor design or technology.
- There is evidence of a correlation between differential pressure around filter and its thickness—the thinner the filter, the more prone to deformation they are and less differential pressure is observed. This phenomena is visible in acoustic response at frequencies >50 Hz.

Both acoustic test campaigns provided a lot of data, which is very useful to validate the computer simulations (e.g., finite element analysis), which will support future design optimizations.

## Acknowledgments

This work was supported by the Polish National Science Centre (Grant No. 2015/18/M/ST9/00541, the ESA PRODEX experiment arrangements, (Grant Nos. PEA 4000124331 and 4000124332), and the Italian Space Agency contract (Grant Nos. 2015-046-R.0, 2018-11.-HH.O and 2019-27-HH.0).

## References

1. K. Nandra, "ATHENA: observing the hot and energetic universe with ESA's next generation x-ray observatory," *Proc. SPIE* **10699**, 106991D (2018).
2. P. Peille et al., "The x-ray integral field unit instrument: science, design, performances and status," *Proc. SPIE* **11444**, 114440V (2020).
3. N. Meidinger et al., "Development status of the wide field imager instrument for Athena," *Proc. SPIE* **11444**, 114440T (2020).
4. M. Barbera et al., "Athena WFI optical blocking filters development status toward the end of the instrument phase-A," *Proc. SPIE* **10699**, 106991K (2018).
5. M. Rataj et al., "The filter and calibration wheel for the ATHENA wide field imager," *Proc. SPIE* **9905**, 990568 (2016).
6. A. Pilch et al., "Acoustic simulation's verification of WFI ATHENA filterwheel assembly," *Arch. Acoust.* **42**(3), 483–489 (2017).
7. M. Van Dyke and J. Hackel, "Theoretical acoustic attenuate on of a random incidence acoustic field through polyester film for various thicknesses as a function of frequency" (2010).
8. W. Hughes et al., "Overview of the acoustic testing of the European Service Module Structural Test Article (E-STA)," in *Conf. Paper from Aerosp. Test. Seminar 2017*, Los Angeles, CA, United States (2017).
9. AGH Laboratory of Technical Acoustics, "'Komora pogłosowa" – description of reverberation room," 2023, <http://www.lat.agh.edu.pl/pomieszczenia/komorapoglosowa/>.
10. R. Lagier, Ariane 6, User's Manual, Arianespace (2018).
11. M. Barbera et al., "Athena WFI optical blocking filters technology readiness assessment at the end of the instrument phase-B," (in preparation).
12. Z. Rarata et al., "Vibro-acoustic response of spacecraft instrument subjected to diffuse sound field: numerical simulations and experimental verification," *Appl. Acoust.* **184**, 108338 (2021).

Biographies of the authors are not available.